FIRST PHYSICS WITH ALICE*

Claus Jørgensen

For the ALICE Collaboration

CERN, Physics Department, 1211 Geneva 23, Switzerland

(Received November 15, 2006)

This paper discusses some aspects of the initial proton–proton physics program with the ALICE experiment at LHC. For initial low luminosity runs ALICE has possibilities comparable to the two dedicated $p+p$ experiments at LHC plus the advantage of a low p_{T} acceptance in the central barrel. It will therefore play an important role in the understanding of the minimum bias proton–proton collisions in the LHC energy regime. The experiment is briefly described and aspects of the initial proton–proton program are discussed in terms of physics, statistics, detector performance and analysis.

PACS numbers: 13.85.Hd

1. Introduction

The main purpose of the ALICE experiment is to measure the properties of the strongly interacting matter created in heavy ion collisions. However, the detector is also capable of making a number of interesting measurements during the initial proton–proton runs when the luminosity has not yet reached the design value of $10^{34}\,\mathrm{cm}^{-2}\mathrm{s}^{-1}$. The full proton–proton program of ALICE includes jet studies, measurements of resonances, photons and heavy flavors and detailed measurements of identified particles spectra [1, 2].

This paper outlines the plans for the first measurements during the pilot runs in late 2007 (at $\sqrt{s} = 0.9$ TeV and perhaps $\sqrt{s} = 2$–2.4 TeV) and in the beginning of 2008 (where the LHC is expected to reach the design energy of $\sqrt{s} = 14$ TeV). The opportunities and limitations given by the ALICE detector systems are described and a number of "day-one" measurements are discussed in the context of previous measurements at lower energies and the theoretical interpretations of these.

* Presented at the "Physics at LHC" Conference, Kraków, Poland, July 3–8, 2006.

2. The ALICE experiment

ALICE is a general purpose experiment with a large number of sub-detectors that cover different acceptance regions. The midrapidity region is covered by an inner tracking system (ITS), a large time projection chamber (TPC) and a number of other detectors for tracking and particle identification (TRD, TOF, HMPID, PHOS, EMCAL). The forward region is covered by detectors for multiplicity measurements and trigger purposes (FMD, VZERO, T0, PMD, ZDC). A spectrometer dedicated for muon measurements covers the forward region on one side of the detector ($-4 < \eta < -2.4$). A detailed description of the detector system and its capabilities can be found in Ref. [1].

For the first measurements one needs to minimize the uncertainty from non-optimal alignment and calibration and these measurements are therefore done with a few independent detector systems. Particle identification in general requires precise calibration and a very good understanding of the detector system and will therefore have a limited scope during the initial runs.

For the day-one measurements ALICE will use the two inner layers of the ITS (the silicon pixel detector SPD), the TPC and the trigger detectors.

2.1. Triggers for day-one physics

The trigger system of ALICE, which is designed for effectively triggering heavy ion collisions, is capable of triggering most of the inelastic proton–proton collisions at high energy. For the proton–proton runs ALICE will use two of the ALICE sub-detectors (SPD and VZERO) in order to form the most effective trigger with the best possible background rejection. The proposed proton–proton minimum bias triggers are sensitive to interactions corresponding to $\approx 90\%$ of the total inelastic cross section (and $\approx 99\%$ of the non-diffractive cross section) and still reject the majority of beam gas interactions [3]. Triggers formed by signals from other detectors (like T0 and TOF) can be used for consistency check and to estimate the systematic uncertainty of the trigger efficiency estimation.

3. The day-one measurements

This section discusses four of the measurements that can be done shortly after the LHC startup: (1) the pseudorapidity density of primary charged particles, (2) the multiplicity distribution, (3) transverse momentum spectra and (4) the mean transverse momentum *versus* multiplicity. The analysis methods that will be used to obtain the results are not discussed here in detail. The physics is discussed in the perspective of measurements at lower energy and in the context of different theoretical ideas and predictions.

3.1. Pseudorapidity density

The pseudorapidity density of primary charged particle at mid-rapidity has traditionally been among the first measurements done with experiments in a new energy domain. Even though the pseudorapidity density around midrapidity is not likely to give direct evidence for new physics it is an important measurement since it gives the first indications of the overall particle production and brings important information for the tuning of MC models.

The pseudorapidity density measured at lower energies seems to be in agreement with a logarithmic dependence on the center-of-mass energy ($\ln(s)$). Such a dependence was hypothesized by Feynman [4] and is often labeled Feynman-scaling. The Feynman-scaling was clearly broken in collisions at the SPS and the multiplicity data including the higher energies seems to follow a $\ln^2(s)$ dependence (like the inelastic or non-diffractive cross-sections).

Figure 1 shows the energy dependence of $dN_{\rm ch}/d\eta|_{\eta\approx 0}$ for inelastic and non-single diffractive collisions at lower energies and the extrapolation to the LHC energy regime (assuming a $\ln^2(s)$ dependence).

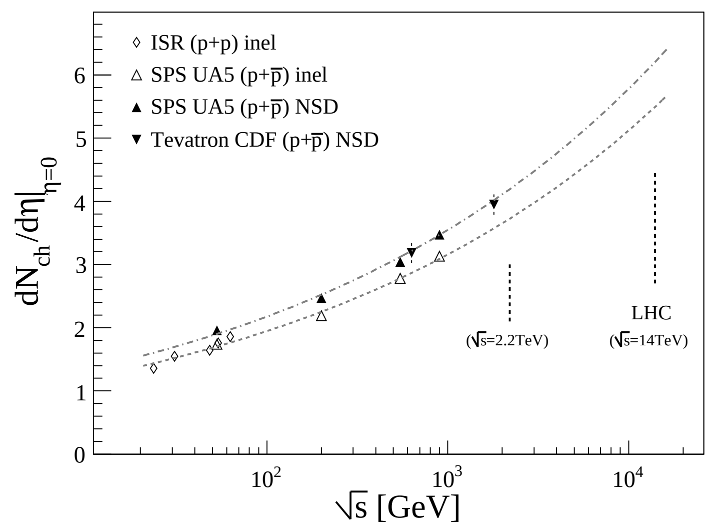

Fig. 1. Center of mass dependence of the pseudorapidity density at midrapidity. Data points are from Ref. [5–7]. The dashed lines show the $\ln^2(s)$ extrapolation to higher energies. The vertical bars indicate the possible LHC energy $\sqrt{s} = 2.2\,\mathrm{TeV}$ and the maximum energy $\sqrt{s} = 14\,\mathrm{TeV}$

ALICE will measure the $dN_{\rm ch}/d\eta$ around midrapidity ($|\eta| < 2$) by counting correlated hits (clusters) in the two layers of the SPD and/or by counting tracks in the TPC. With the expected low multiplicity in proton–proton events, the occupancy in the highly segmented detectors will be very low and corrections for detector inefficiency and contamination will be applied only as function of the pseudorapidity and z-position of the collision vertex. The measurement can be done with very few events (10^4 events will give a statistical error of $\approx 2\%$ for bins of $\Delta\eta = 0.2$ assuming $dN_{\rm ch}/d\eta|_{\eta\approx 0} = 6$).

Extending the measurement to a larger pseudorapidity range using the forward detector systems ($2 < |\eta| < 5$) is more complicated since it requires good understanding of the secondary particle production which becomes the dominant source of charged particles at lower angles.

3.2. Multiplicity distribution

The multiplicity distribution, *i.e.* the probability P_n of producing n primary charged particles in a collision, will be among the first measurements done with ALICE.

At lower energies the data seems to follow KNO-scaling according to which the multiplicity distributions scales with the mean multiplicity and follows a universal function ($P_n = \langle n\rangle^{-1}\phi(n/\langle n\rangle)$) [8]. The theoretical basis for such a scaling is discussed in Ref. [9]. At higher energies (above ISR), the KNO-scaling is clearly broken [10], which is understood in terms of (coherent) particle production from hard scattering (jets and mini-jets production) or from the effect of multiple parton interactions in the same proton–proton collision. Thus, measurements of the multiplicity distributions (in different η-ranges) will bring the first indication on the importance of multiple parton interactions and the interplay between soft (low multiplicity) and hard (high multiplicity) processes in the new energy regime.

Experimentally the multiplicity distribution is not straightforward to extract, which perhaps explains the inconsistency of measurements at lower energies (for example, the multiplicity distributions at $\sqrt{s} = 546\,\mathrm{GeV}$ from E735 and UA5 differ by more than a factor of two above $N_{\rm ch} \approx 80$ [11]). The detector response matrix, *i.e.* the probability that a certain true multiplicity gives a certain measured multiplicity, can be obtained from detector simulation studies. From this and the measured spectrum, the true multiplicity spectrum can be estimated using different unfolding techniques [12, 13].

The statistics used for these measurements have not been high at lower energies (6839 events were used by UA5 in Ref. [13] giving a multiplicity spectrum for $\eta < 1.5$ with the highest bin of $58 < N_{\rm ch} < 76$). It is expected that the measurement at $\sqrt{s} = 900\,\mathrm{GeV}$ can be extended significantly — 10^6 events (which can be recorded within 3 hours when running at 100Hz) will enable to extend multiplicity spectrum up to $N_{\rm ch} \approx 100$. At $\sqrt{s} = 14\,\mathrm{TeV}$ the measurements are expected to reach (according to PYTHIA) $N_{\rm ch}^{\eta<1.5} > 250$ with 10^6 events.

3.3. Transverse momentum spectra

The transverse momentum spectrum of primary charged particles emitted in proton–proton collisions will also be one of the first measurements of ALICE.

At high p_{T}, the transverse momentum spectra are well described by LO or NLO pQCD calculations, but this approach still depends on phenomenological parameters and functions (K factor, parton distribution function and fragmentation functions), which needs to be determined experimentally. At lower p_{T}, where perturbative QCD cannot be applied, the models rely on an even more insecure theoretical foundation.

Early measurements of p_{T} spectra are important for the tuning of the model parameters and for the understanding of background in experimental study of more rare processes. Also, the measurement of the p_{T} spectrum is important for the understanding of jet quenching studies in heavy ion collisions, where the proton–proton data is used as reference.

Figure 2 shows p_{T} spectra of charged particles at different energies. The high p_{T} yield rises dramatically with the collision energy due to the increase of the hard processes cross sections.

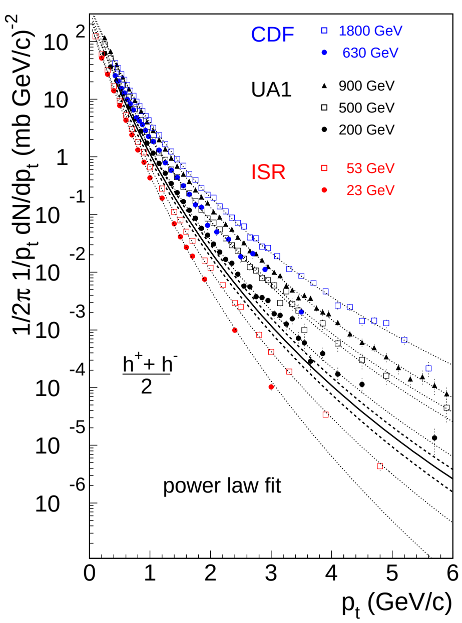

Fig. 2. Midrapidity transverse momentum spectra of unidentified hadrons at different energies. The plot is from Ref. [14].

The p_{T} spectrum is obtained by counting the number of tracks in each p_{T} bin and correcting for the detector and reconstruction inefficiencies (as function of z, η and p_{T}). The p_{T} distribution is in the end normalized by the number of collisions and corrected for the effect of vertex reconstruction inefficiency and trigger bias.

With an event sample of 10^6 events ALICE can extend the UA1 measurement at $\sqrt{s} = 900\,\mathrm{GeV}$ and reach $p_{\mathrm{T}} > 15\,\mathrm{GeV}/c$. With 10^6 events at $\sqrt{s} = 2.2\,\mathrm{TeV}$ ALICE could reach $p_{\mathrm{T}} \approx 20\,\mathrm{GeV}/c$ and at $\sqrt{s} = 14\,\mathrm{TeV}$ $p_{\mathrm{T}} > 40\,\mathrm{GeV}/c$ (according to PYTHIA).

3.4. Mean transverse momentum versus multiplicity

The balance between particle production and the transverse energy of the produced particles is reflected in the multiplicity dependence of the mean transverse momentum. At lower energies the mean transverse momentum is growing with the charged particle multiplicity [15, 16], which can be understood in terms of jet production (the energy transfer between the two hard-scattered partons is shared between particle production and the transverse energy). Since high multiplicity jets have a high mean p_{T} it could be expected that also high multiplicity events would have higher mean p_{T}. However, the CDF Collaboration has demonstrated that the rise of the mean p_{T} with multiplicity is also present in events with no jets (for definition of "no jets", see Ref. [16]).

Detailed measurements of the mean p_{T} *versus* multiplicity will thus give the first insight to the jet fragmentation process and the underlying event structure.

Once the multiplicity distribution and the p_{T} spectra have been measured, it becomes relatively straightforward to obtain the correlation between the mean p_{T} and the multiplicity. Estimating the mean p_{T} over the full p_{T} range will be attributed with a relatively large systematic uncertainty stemming from the p_{T} cut-off imposed by the detector — this is also the reason why earlier measurements often quote the mean p_{T} for particles above a certain p_{T} threshold. ALICE has a p_{T} cut-off of $\approx 100\,\mathrm{MeV}/c$ for pions and $\approx 300\,\mathrm{MeV}/c$ for protons.

4. Summary and outlook

During the initial LHC runs with proton–proton collisions, ALICE will focus on minimum bias measurements where it will be able to compete with the dedicated proton–proton experiments at LHC. In this paper four of the "day-one" measurements have been outlined and discussed briefly. These are likely to be the first physics measurements published by ALICE. Later, when a more precise alignment and calibration (and understanding of the detector) is achieved, ALICE will perform more detailed measurements of proton–proton collisions. More details can be found in reference [1, 2].

REFERENCES

[1] ALICE Collaboration, TDR `http://aliceinfo.cern.ch/Collaboration/Documents/TDR/index.html`; PPR Vol. I, *J. Phys. G: Nucl. Part. Phys.* **30**, 1517 (2004); PPR Vol. II, *J. Phys. G: Nucl. Part. Phys.* **32**, 1295 (2006).

[2] J.P. Revol, *Pramana* **60**, 795 (2003).

[3] J. Conrad, G. Contreras, C. Jørgensen, Internal note, ALICE-INT-2005-025.

[4] R. Feynman, *Phys. Rev. Lett.* **23**, 1415 (1969).

[5] W. Thome, *et al.*, *Nucl. Phys.* **B129**, 365 (1977).

[6] G.J. Alner *et al.*, *Z. Phys.* **C33**, 1 (1986).

[7] F. Abe *et al.*, *Phys. Rev.* **D41**, 2330 (1990).

[8] Z. Koba, H.B. Nielsen, P. Olesen, *Nucl. Phys.* **B40**, 317 (1972).

[9] P. Slattery, *Phys. Rev. Lett.* **23**, 1415 (1969); E.H. de Groot, *Phys. Lett.* **B57**, 159 (1975); Lian-sau, Ta-Chung, *Phys. Rev.* **D27**, 2640 (1983).

[10] *G.J. Almer et al.*, *Phys. Lett.* **138B**, 304 (1984).

[11] T. Alexopoulos *et al.*, *Phys. Lett.* **B435**, 453 (1998).

[12] V.B. Anykeev *et al.*, *Nucl. Instrum. Methods* **A303**, 350 (1991); G. d'Agostini, DESY 94-099, June 1984.

[13] R.E. Ansorge *et al.*, *Z. Phys.* **C43**, 357 (1989).

[14] A. Drees, *Nucl. Phys.* A698, 331 (2002).

[15] G. Arnison]*et al.*, *Phys. Lett.* **118B**, 167 (1982).

[16] D. Acosta *et al.*, *Phys. Rev.* **D65**, 027005 (2002).